Hydrothermal Desorption of Cs with Oxalic Acid from Hydrobiotite and Wastewater Treatment by Chemical Precipitation

Sung-Man Kim [1,2] **, In-Ho Yoon** [1,*] **, Ilgook Kim** [1] **, June-Hyun Kim** [1] **and So-Jin Park** [2,*]

[1] Decommissioning Technology Research Division, Korea Atomic Energy Research Institute, 989-111, Daedeokdae-ro, Yuseong-gu, Daejeon 34057, Korea; smkim32@kaeri.re.kr (S.-M.K.); ilgook@kaeri.re.kr (I.K.); kjh0725@kaeri.re.kr (J.-H.K.)

[2] Department of Chemical Engineering and Applied Chemistry, College of Engineering, Chungnam National University, 99 Daehak-ro, Yuseong-gu, Daejeon 34134, Korea

* Correspondence: ihyoon@kaeri.re.kr (I.-H.Y.); sjpark@cnu.ac.kr (S.-J.P.); Tel.: +82-42-868-8281 (I.-H.Y.); +82-42-821-5684 (S.-J.P.)

Abstract: A hydrobiotite (HBT) clay contains more cesium (Cs)-specific adsorption sites than illitic clay, and the capacity of frayed edge sites can increase as the weathering of micaceous minerals proceeds. Thus, Cs can be selectively adsorbed to HBT clay. In this study, we investigated the removal efficiency of non-radioactive (^{133}Cs) and radioactive (^{137}Cs) Cs from HBT, using oxalic acid. We found the minimum optimal concentration of 0.15 M oxalic acid removed more than 90% of Cs. Subsequently, cations and Cs ions were removed using Ca(OH)$_2$ and sodium tetraphenylborate (NaTPB) to treat the washing wastewater generated at the optimum concentration of the desorbent (0.15 M oxalic acid). In order to remove cations and heavy metal ions in the waste solution, Ca(OH)$_2$ was treated at a mass ratio of 0.025 g/mL and pH 9–10 to derive optimal conditions. As a final step, to remove Cs, NaTPB was treated with a mass ratio of 2 mg/mL and reduced to below 0.1 mg/L Cs to find the optimal dose. The novelty of this study is that the amount of radioactive waste can be drastically reduced by removing the non-radioactive cations and heavy metals separately in the first step and removing the remaining radioactive Cs in the second step.

Keywords: hydrobiotite (HBT); oxalic acid; cesium; chemical precipitation; wastewater treatment

1. Introduction

The widespread radioactive contamination following the 2011 Fukushima nuclear power plant disaster has spurred research on the removal of radionuclides from soil to reduce radioactivity in contaminated areas. To date, cesium (Cs) remains the most concerning radionuclide due to its strong affinity with clay minerals in soil and the fact that it continues to accumulate in topsoil [1,2]. In particular, Cs ions interact strongly and selectively with 2:1 phyllosilicate clay minerals such as smectite, vermiculite, and illite [3,4]. Cesium is generally adsorbed to the interlayer of these clay minerals, and irreversible adsorption occurs in the frayed edge sites (FES) and is barely removed by conventional soil treatment methods.

Among the clay minerals, hydrobiotite (HBT), which is composed of interstratified layers of vermiculite and biotite, is generally produced during the weathering of biotite to vermiculite [5,6]. Yamada et al. (2014) reported that the Cs adsorption capacity of clay increased with the degree of biotite weathering [7]. Nakao et al. (2008) observed that vermiculitic clay contained more Cs-specific adsorption sites than illitic clay based on radiocesium interception potential analysis, and the capacity of FES can increase as the weathering of micaceous minerals proceeds [8]. It was also reported that

partially weathered biotite found in Fukushima soil could selectively adsorb Cs in the presence of other clay minerals such as smectite [9], and it can be a major Cs adsorbent in Fukushima soil [10,11].

Oxalic acid is a chelating agent with a carboxyl group that can bond to metal ions such as Al or Mg in crystals of a clay mineral. It releases metal ions to form a metal−oxalate complex, and in this way, the crystals of clay minerals can be destroyed [12–14]. This reaction can accelerate the release of Cs from clay to which Cs ions have been adsorbed on the surface and the FES. In particular, HBT is capable of expanding between layers, and it easily desorbs Cs due to ion exchange. Therefore, this reaction is more pronounced than with non-expandable clay minerals.

In order to remove Cs from vermiculite-type clay minerals, decontamination experiments using acid treatment or ion exchange have been variously attempted. One paper reported that cationic surfactant and cationic polyelectrolyte effectively desorbed Cs from HBT via ion exchange [15]. Cs adsorption/desorption experiments with various clay minerals from Fukushima were also investigated, and only 58% of ^{137}Cs in weathered biotite was desorbed by 1 M hydrochloric acid [11]. Although many researchers have reported the Cs desorption behavior from vermiculite and micaceous clay minerals, the removal of Cs from clay minerals remains challenging, and the desorption of Cs from HBT has not yet been successfully investigated.

Added to this, a large amount of washing wastewater is generated after decontamination of Cs contaminated soil using acid treatment. Radioactive liquid waste contaminated with ^{137}Cs radionuclides must be treated effectively due to its long half-life, high solubility/mobility, and high radiotoxicity. Various chemical, physical, biological and combined methods have been developed to decontaminate radioactive wastewater. Among them, physicochemical methods include adsorption and ion exchange, advanced oxidation process, and chemical precipitation [16]. In addition, electrochemical methods have been studied, such as electrodialysis, electro-adsorption and electrodeionization to decontaminate radioactive wastewater [17]. Additionally, membrane has shown great potential for decontamination of radioactive wastewater due to its unique pore-sized-dependent separation mechanism. The methods include reverse osmosis, nanofiltrtion, membrane distillation, and forward osmosis [18]. Among the various methods to treat radioactive liquid waste, chemical precipitation is an effective and the most widely used process in industry, because it is relatively simple and inexpensive to conduct [19]. In the precipitation process, chemicals (Ca(OH)$_2$) react with metal ions to form insoluble precipitates, and Cs also reacts with precipitants (NaTPB) to form insoluble salt precipitates. The forming precipitates can be separated from the water by sedimentation or filtration which resulted in the reduction of radioactive waste volume [20].

In this study, we measured the efficiency of the removal of non-radioactive (^{133}Cs) and radioactive (^{137}Cs) Cs at different concentrations from a slightly expandable clay (HBT), using oxalic acid. In addition, in order to investigate the desorption properties, we analyzed the structural change using X-ray diffraction (XRD) and the change in the metal ion release amount according to the concentration of oxalic acid treatment. In the wastewater treatment process, we purified the wastewater through a two-step process to remove metal ions and Cs ions. In the first step, hydroxide precipitation using Ca(OH)$_2$ was treated to remove metal ions, and in the second step, Cs ions were removed by treatment with sodium tetraphenylborate (NaTPB). We found the optimal dosage to remove metal ions and Cs from oxalic acid washing wastewater and investigated the optimum pH range of the solution, and we confirmed that the Cs and metal ions were significantly reduced by the two-step treatment.

2. Materials and Methods

2.1. Materials

The HBT (Sigma-Aldrich) used in this study was ground in a milling machine and sieved to achieve a particle size below 20 μm, and air-dried at room temperature. The CsCl used in the adsorption experiments was from Sigma-Aldrich. Oxalic acid dihydrate (Sigma-Aldrich, Germany) was used as the desorbent to remove Cs from clay minerals. Calcium hydroxide (*Mw* = 74.06 g/mol, assay 96%,

Junsei Chemical Co., Ltd, Tokyo, Japan) and sodium tetraphenylborate (*Mw* = 342.22 g/mol, assay 99.5%, Junsei Chemical Co., Ltd, Tokyo, Japan) were used to purify the washing wastewater contaminated with Cs and metal ions after the desorption experiment.

2.2. Adsorption and Hydrothermal Desorption of Non-Radioactive [133]Cs–HBT

The HBT (35 g) was mixed with an aqueous solution of 3 mM CsCl (350 mL) in a polypropylene bottle, and the mixture was equilibrated at room temperature for 7 d on a horizontal shaker. The Cs-adsorbed HBT ([133]Cs–HBT) was then separated and washed twice in deionized water by resuspension and centrifugation, then dried at 70 °C for 24 h. The concentration of Cs in the aqueous phase was analyzed using inductively coupled plasma mass spectroscopy (ICP-MS; ELAN DRC II, PerkinElmer, USA), and the amount of Cs adsorbed on the clay was found to be 3.896 mg/g (=29.29 mmol of Cs/kg clay).

For the [133]Cs desorption experiments, we variously added 0.015, 0.15, 1, and 1.5 M oxalic acid (35 mL) to the [133]Cs–HBT (0.35 g) in a 60 mL polypropylene tube. The reaction was carried out in a shaking heating bath (BS-21; JeioTech, Korea) at 70 °C for 2 d to facilitate thermal desorption. The solid/liquid was then separated by centrifugation (Combi-514R multi-purpose centrifuge; Hanil Science Inc., Korea) at 4000 rpm for 15 min, and the supernatant was collected and filtered through a polyvinylidene fluoride membrane filter (pore size = 0.45 μm). The concentration of Cs desorbed from the clay was determined using ICP-MS.

2.3. Adsorption of Radioactive ^{137}Cs to HBT and its Desorption by Oxalic Acid

Radioactive ^{137}Cs-adsorbed hydrobiotite (^{137}Cs–HBT) was prepared by mixing 20 g HBT with a 200 ml ^{137}Cs solution (35 Bq/mL) for 7 d at room temperature. After separation of the ^{137}Cs–HBT by centrifugation and washing with deionized water, the radioactive HBT was dried at 40 °C, and the radioactivity of the aqueous phase containing the unabsorbed ^{137}Cs was analyzed using a multi-channel analyzer (MCA; CANBERRA Ind, Meriden, CT, USA) equipped with a high-purity germanium detector, to assess the ^{137}Cs radioactivity level of the HBT. The radioactivity of the obtained ^{137}Cs–HBT was 327 Bq/g (= 0.75×10^{-6} mmol of Cs/kg clay). The adsorption concentration of radioactive ^{137}Cs–HBT was adsorbed above the level that can be released in an actual nuclear accident in order to meet the self-disposal standard of radioactive waste (0.1 Bq/g).

For the desorption experiments, 350 mg of ^{137}Cs–HBT (327 Bq/g) was variously mixed with 0.015, 0.15, 1, and 1.5 M oxalic acid solution (35 mL) at 70 °C. After 2 d of reaction, the samples were centrifuged for solid/liquid separation. The radioactivity of the supernatant, filtered through a polyvinylidene difluoride membrane filter (pore size = 0.45 μm) was measured using the MCA to quantify the amount of ^{137}Cs desorbed [21].

2.4. Characteristics of Cs-Desorbed Soil

In order to investigate the Cs desorption properties, we analyzed the change in the release amount of metal ions according to the concentration of oxalic acid treatment. To analyze the chemical composition of the HBT, we used X-ray fluorescence (XRF) analysis (Rigaku ZSX Primus II; Japan) equipped with an end-window 3 kW Rh X-ray tube, and a scintillation counter and a gas flow proportional counter were used as detectors. To prepare a double-layer pellet, a HBT mass of 200 mg was pressed onto a boric acid backing pellet (6 g) in an aluminum cup (Φ40 mm) using a pressure of 20 tons. The sample preparation for XRD involved initial solid/liquid separation by centrifugation, drying of the solid at 60 °C to remove water, then grinding the dried sample to fine particles using a mortar and pestle. The XRD patterns of Cs–HBT exposed to various oxalic acid concentrations were obtained using a Rigaku Smart Lab diffractometer (Japan) with CuKa radiation (λ = 1.54 nm). Data were collected in the range of 2θ = 2–30° with a step size of 0.02° and at 2 s/step. Samples of oxalic acid-treated Cs–HBT were prepared by drying at 60 °C. Following treatment with oxalic acid, we analyzed the changes in morphology and composition of HBT using a low voltage field

emission scanning electron microscope (FE-SEM; Zeiss Merlin; resolution 0.8 nm at 15 kV). In addition, the surface area and pore volume were measured using Brunauer–Emmett–Teller (BET, ASAP 2010 Micrometrics Analyzer) equipment for microstructure analysis. Nitrogen adsorption isotherms were obtained at liquid nitrogen temperature.

2.5. Washing Wastewater Treatment Using Chemical Precipitation

The optimum condition for obtaining more than 90% Cs removal efficiency at 0.15 M oxalic acid was derived from both radioactive and non-radioactive experiments. Thus, we experimented to find the optimal dosage and pH range of $Ca(OH)_2$ and NaTPB in washing wastewater of 0.15 M oxalic acid. First, in order to find the optimal dose of $Ca(OH)_2$, the washing wastewater reacted at 0.15 M of oxalic acid and $Ca(OH)_2$ was mixed at different mass ratios (0.1, 0.3, 0.5, 0.7, 0.9, and 1.2 g $Ca(OH)_2$/15 ml oxalic acid washing wastewater) and reacted overnight at 25 °C in a shaking incubator. Different pH levels were measured according to the dose of $Ca(OH)_2$. The following day, the precipitate was discarded by solid/liquid separation, the supernatant was filtered through a polyvinylidence difluoride (PVDF) membrane filter (pore size = 0.45 μm), and the concentration of cations was measured using ICP-MS. Secondly, in order to find the optimal dosage and pH range of NaTPB, the cation-depleted 0.15 M oxalic acid washing wastewater and NaTPB were mixed at different mass ratios (2.5, 5, 10, 15, 20, and 25 mg NaTPB/10 mL oxalic acid washing wastewater) and reacted overnight at 25 °C in a shaking incubator. Then, the pH of solution was not adjusted after adding NaTPB, because the pH 12 was adjusted by the previous step. The following day, the precipitate was discarded by solid/liquid separation, the supernatant was filtered through a PVDF membrane filter (pore size = 0.45 μm), and the concentration of ^{133}Cs ions was measured using ICP-MS. In addition, the pH of oxalic acid washing wastewater was prepared at pH 1, 3, 5, 7, 9, 11, and 13 solution in order to find the optimum pH range. An amount of 20 mg NaTPB was added to 10 ml washing wastewater prepared at various pH, and then the mixture was reacted overnight at 25 °C in a shaking incubator. The following day, precipitate separation and ^{133}Cs ion concentration analysis were conducted in the same way as the above process.

The optimum dose and pH conditions of $Ca(OH)_2$ and NaTPB that we found were actually applied to the washing wastewater after the oxalic acid desorption experiment from 0.015 to 1.5 M concentration. In the first step to remove cations from the desorption wastewater, $Ca(OH)_2$ was treated at a mass ratio of 0.025 g/mL, and the pH was adjusted from 9 to 10. The following procedure was the same as the above method. In the second step, 2 mg/mL NaTPB was added to the cation-depleted wastewater in the previous step to remove Cs in the solution, and the pH was adjusted to 12. The mixture was stirred overnight at 25 °C in a shaking incubator. The following procedure was the same as the above method. Figure 1 is a schematic diagram showing the entire process of a soil washing process using oxalic acid of Cs–HBT and a wastewater treatment process using a chemical precipitation method.
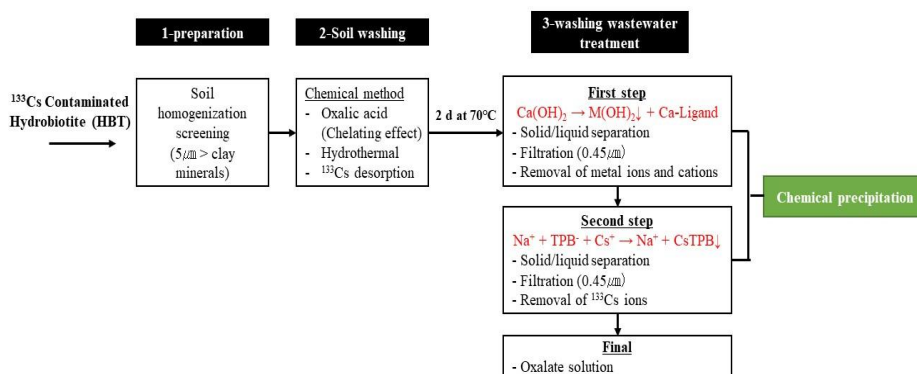

Figure 1. Schematic diagram of soil washing and washing wastewater treatment of cesium (Cs)-contaminated hydrobiotite (HBT).

3. Results and Discussion

3.1. Cs Desorption by Oxalic Acid from HBT Contaminated with ^{133}Cs and ^{137}Cs

The efficiencies of oxalic acid desorption of Cs were compared in experiments conducted at 70 °C for 2 days in a shaking heating bath. The desorption efficiency improved with increasing desorbent concentration; the maximum efficiency for Cs desorption in both the radioactive and non-radioactive experiments was 99.05% and 98.45% at 1.5 M, respectively (Figure 2).
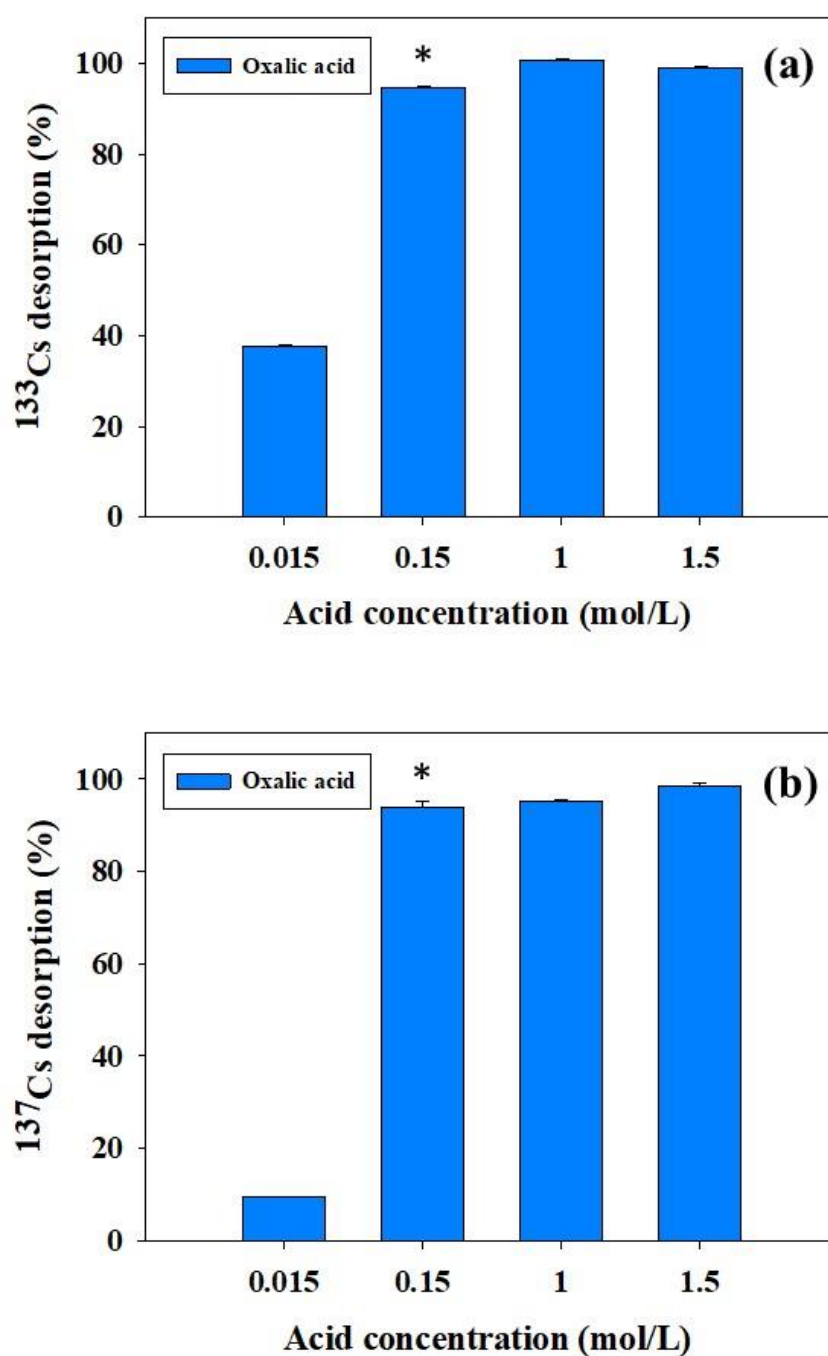
Figure 2. Removal efficiency of (**a**) non-radioactive (^{133}Cs) and (**b**) radioactive (^{137}Cs) cesium from HBT at various concentrations (0.015–1.5 M) of oxalic acid at 70 °C for 2 d. (n = 3, mean ± standard error of mean). * Optimal dosage concentration of oxalic acid.

Positively, starting with a concentration of 0.15 M oxalic acid desorbent, a Cs removal efficiency above 90% was obtained in both the radioactive and non-radioactive experiments. From these experimental results, we found the optimum conditions to treat the minimal desorbent on 0.15 M oxalic acid, indicating that acid treatment of HBT resulted in effective Cs desorption. Komadel and Madejová (2013) reported that the acid treatment of clay minerals partially dissolves a clay crystalline structure by leaching cations including Mg, Al, and Fe from the octahedral sheet, and that Cs leaches too [22]. In addition, acid treatment of clay minerals increases the surface acidity, specific surface area, and porosity [23,24]. In the case of HBT, the solution pH is lower due to acid treatment, and the weathering and dissolving of clay minerals is more active [25,26]. Thus, these active actions swell between the layers of HBT and maximize the chelating effect of oxalic acid. The oxalic acid chelation accelerates the dissociation of Cs through the leaching of metal ions between layers, formation of oxalate metal complexes, and structural changes [12–14]. Thus, it appears that oxalic acid can desorb Cs adsorbed onto the interlayer and FES (irreversible site), explaining the higher removal efficiency of oxalic acid. The desorption of Cs from soil using acid treatment has been widely studied. Soil from a decommissioned nuclear production complex in the USA (Hanford, Washington) was reacted with $(NH_4)_2$-oxalate for 68 d, and a desorption efficiency of 63% was achieved [27]. For contaminated soil associated with the TRIGA nuclear reactor program (Republic of Korea), 50% desorption efficiency was obtained using oxalate [28]. Wendling et al. (2004) reported that 55% of Cs was removed from illite by oxalate solution. In contrast to these previous studies, in this study, desorption experiments were conducted using oxalic acid in HBT, a slightly expandable clay, and at the same time, hydrothermal treatment was performed at 70 °C for 2 days. These methods help to desorb Cs between layers and increase efficiency [29].

3.2. The Release of Al, Fe, Mg, and Si from [133]Cs–HBT by Oxalic Acid

The [133]Cs–HBT was incubated for 2 d in various concentrations (0.015, 0.15, 1, and 1.5 M) of oxalic acid. The concentrations of the major elements released from [133]Cs–HBT, including Al, Fe, Mg, and Si, were monitored to estimate the degree of simultaneous dissolution of clay minerals. As shown in Figure 3, the extraction efficiency of elements was improved by increasing the desorbent concentration. From 0.15 M of the desorbent (oxalic acid), the leaching of cations began to increase, and among the major elements of HBT, Mg (1389.60 mg/L) leached most, followed by Fe (687.25 mg/L), Al (578.90 mg/L), and Si (262.50 mg/L).

During the weathering process, biotite causes hydrogen ions or cations in the solution to be replaced with K^+ ions between layers. K^+ ions were substituted with Mg^{2+} ions to form vermiculite [30–32]. Some explanations can be found in studies that affirm that Mg rich clays are more easily attacked by acids and the octahedral sheets easily undergo leaching. Due to its larger specific surface areas and more edges, HBT is more easily attacked by acids [33]. The results of our experiments were reported similarly by Wang et al. (2005), who reported that the amount of Si and Al that leached from kaolinite was highest using oxalic acid [34]. In several studies of the cation leaching mechanism during organic acid enhancement of kaolinite dissolution, the results indicated that organic acid anions could complex with Al on the kaolinite surface and promote its dissolution [35,36]. This also indicates that the effect of organic acids on clay minerals involves a combination of acid attack and chelation.

We performed solid/liquid separations following the desorption reactions, and analyzed the solid phases using XRF. Table 1 shows the cation release data, comparing the major element content of clay minerals following desorption. The amounts of Mg, Al, Fe, and K decreased with increasing treatment time of oxalic acid, indicating that these cations were partially dissolved from the [133]Cs–HBT layer by treatment of oxalic acid. Previous studies reported that oxalate ligands have a strong complexing ability as a result of interaction with cations, and are effective in partially dissolving the cations bonded to Cs [37,38]. Thus, this study supports the experimental findings of increased desorption efficiency and leaching of [133]Cs from HBT associated with cation leaching.
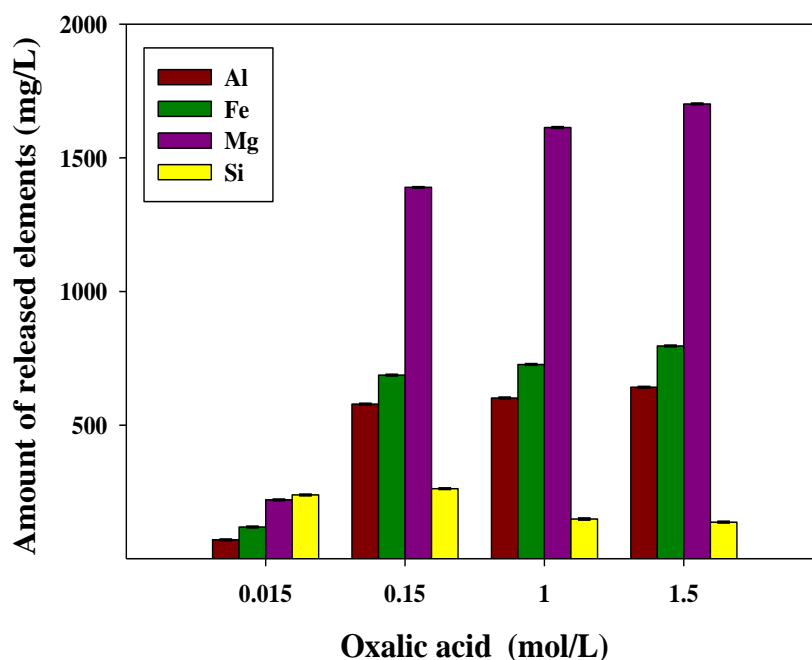
Figure 3. The amount of major elements released following oxalic acid desorption of Cs-adsorbed HBT ([133]Cs–HBT), used to estimate the degree of dissolution of clay compounds: Al, Fe, Mg, and Si. (n = 3, mean ± standard error of mean).

Table 1. Quantification using elemental information from the X-ray fluorescence (XRF) analysis (%).

Clay	ConcenTration (mol/L)	Reaction Time	MgO	Al_2O_3	SiO_2	K_2O	TiO_2	Fe_2O_3
HBT	Raw-HBT	D.W.	25.53 ± 0.03	11.81 ± 0.02	43.44 ± 0.05	6.30 ± 0.25	1.18 ± 0.01	8.05 ± 0.02
	Oxalic acid 1 M	1 day	2.70 ± 0.00	2.14 ± 0.00	90.30 ± 0.09	0.65 ± 0.04	0.27 ± 0.02	1.06 ± 0.05
		2 days	2.50 ± 0.15	1.73 ± 0.58	90.00 ± 0.89	0.60 ± 0.02	0.22 ± 0.00	0.89 ± 0.05

3.3. Structural and Morphological Effects of Oxalic Acid Treatment on [133]Cs–HBT

Figure 4 shows the structural changes in HBT following treatment for 2 days with oxalic acid, analyzed using XRD. The XRD reflection intensities for the raw-HBT specifically reveal the main characteristic peaks at 2θ = 6.2°, 7.3°, and 8.7°, corresponding to interlayer spacings of 14.0 Å, 12.0 Å, and 10.1 Å, respectively. At the lowest oxalic acid concentration, 0.015 M, a major characteristic peak similar to raw HBT was shown. However, it was confirmed that the reflection intensity weakened or disappeared in the typical peak of HBT in the increase in oxalic acid treatment concentration. In addition, peaks with very weak reflection intensity were observed at the treatment concentrations of 0.15 M and 0.2 M oxalic acid, which appeared at 2θ = 8.81° (10.02 Å) and 8.86° (9.96 Å). Then, the peaks of HBT disappeared completely from 0.5 to 1.5 M oxalic acid, and it was confirmed that the peaks after 2θ = 15° were oxalic acid components, which remained in precipitation of the soil (solid samples). It was seen that the reflection intensity of oxalate becomes stronger as the treatment concentration increases. These results are similar to those of Mukai et al. (2018). After treatment with 1 M NH_4NO_3, 1 M KNO_3, and 1 M $CsNO_3$ solution using weathered biotite collected from Fukushima, the structure change was observed by XRD analysis. The peak after 2θ = 10° had disappeared, and the peak at 2θ = 5.8° had completely disappeared when the solution of 1 M HNO_3 and 1 M HCl was treated [39]. Thus, previous reports of XRD reflection intensity where peaks have weakened or disappeared, suggest that acid treatment causes the weathering of clay minerals. In particular, HBT has a more pronounced effect on acid treatment than non-expandable clay minerals. As a result, after acid treatment, pores are formed at the edges of the HBT, curling occurs at the edges, and the HBT finally

becomes an amorphous structure. Therefore, the surface area and pore volume were measured using BET analyzer for the microstructure analysis before and after treatment of oxalic acid with Cs–HBT. The BET surface area in the raw sample was 5.84 m^2/g and 153.06 m^2/g in oxalic acid treated Cs–HBT. In addition, the single point adsorption total pore volume of the raw sample was 0.03 cm^3/g and the oxalic acid-treated Cs–HBT was 0.23 cm^3/g. These results are caused by weathering and cracking of the edges due to acid treatment.
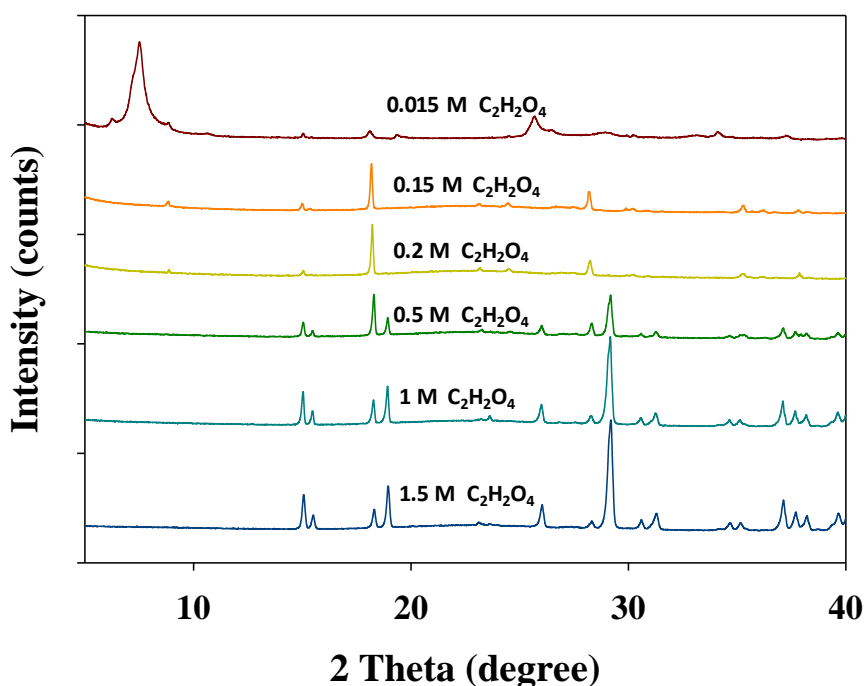
Figure 4. X-ray diffraction (XRD) patterns of [133]Cs–HBT treated with various concentrations of oxalic acid. The solid/liquid samples were separated using a centrifuge following desorption treatment, and the dried solid particles were analyzed using XRD.

The corresponding SEM micrographs and energy dispersive spectroscopy (EDS) analysis are shown in Figure 5. Clear morphological changes were observed in the SEM image of HBT after acid treatment. Figure 5A–C show the typical morphology and EDS-elemental mapping of the untreated, slightly expanded clay (HBT). Figure 5D–F show the morphology and EDS-elemental mapping of the changed surface of HBT after 1.5 M treatment with oxalic acid. The raw-HBT was observed to have a unique sheet texture and smooth foundation surface at the edges, with no significant change.

The HBT treated with 1.5 M oxalic acid has weathered and sharpened edges due to the release of cations (Al, Si, K and Fe). Furthermore, the surface was broken due to the dissolving of the edges, and broken debris was scattered around [40,41]. EDS-elemental mapping confirmed the elution of cations after acid treatment. Because Si was released at the plate edge, the Si concentration was an indicator related to the HBT weathering, and the K release from the interlayer was related to ion exchange rather than plate dissolution [40,42,43]. Thus, organic acid (oxalic acid) seems to dissolve cations in the layer, weakening the minerals, destroying the layer structure, and affecting the elution of Cs [44].
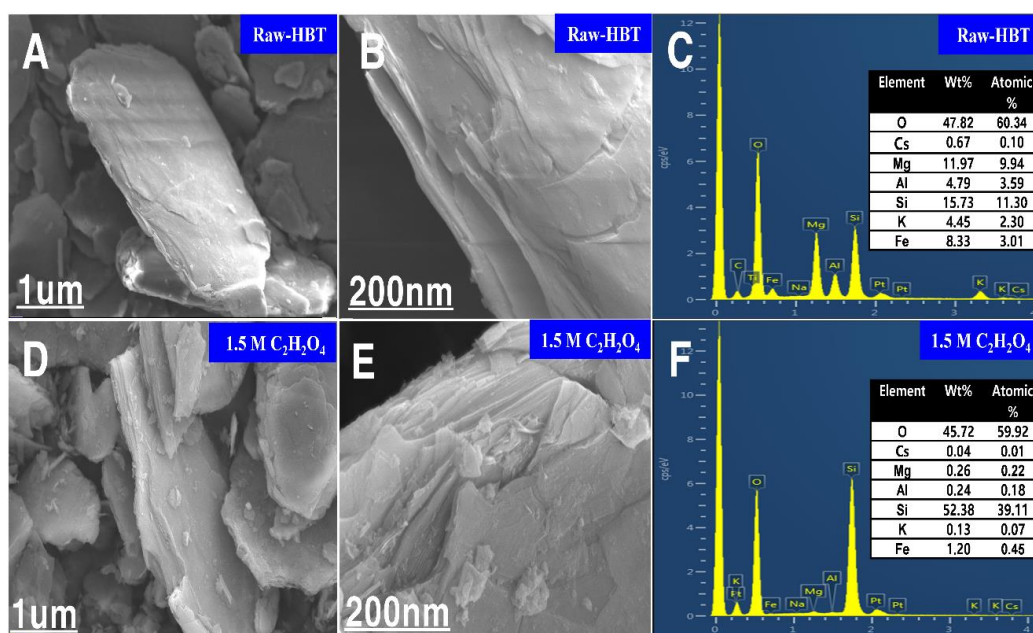
Figure 5. The results of scanning electron microscope (SEM)–energy dispersive spectroscopy (EDS) analysis of the solid sample after the desorption experiment. The SEM imaging shows: (**A**,**B**) Raw-HBT; (**D**,**E**) after 1.5 M oxalic acid treatment. (**C**) and (**F**) are the EDS-mapping.

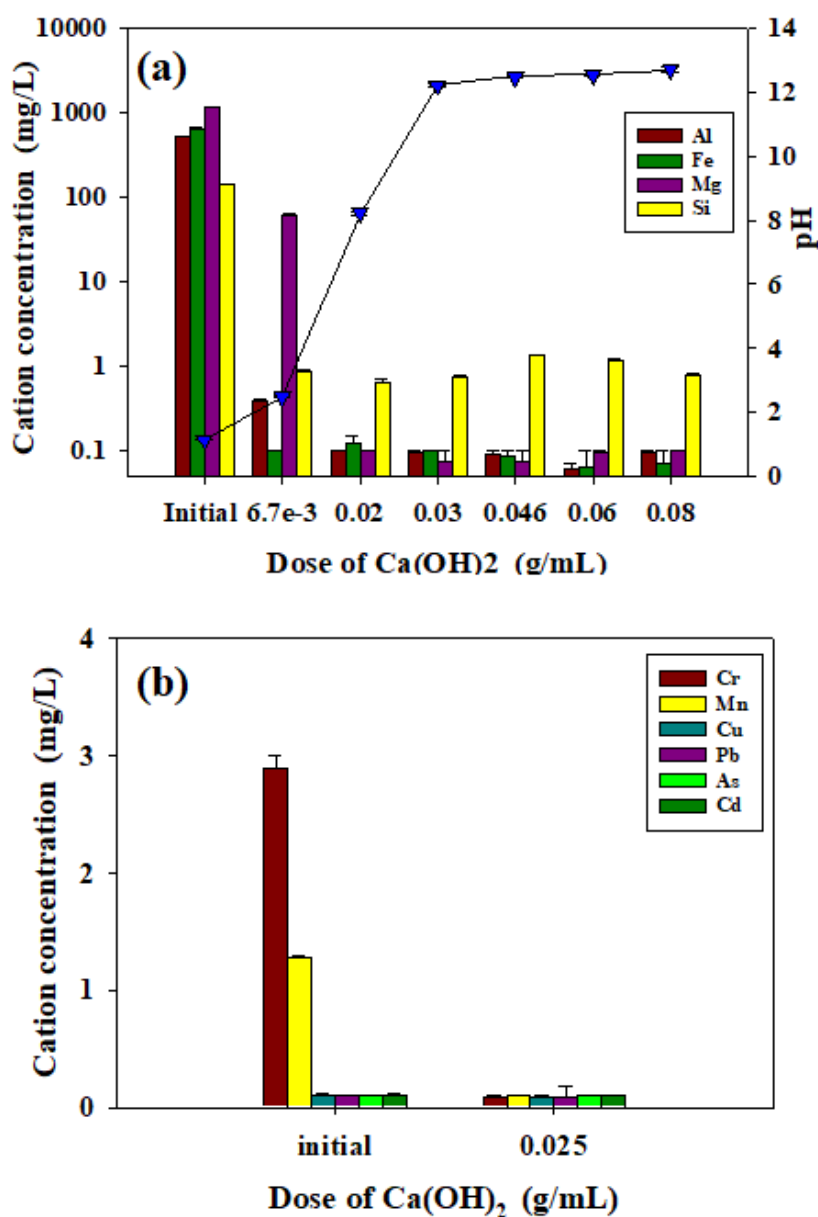### 3.4. Removal of Cations from Washing Wastewater of ^{133}Cs–HBT

We found the optimal treatment conditions for cations and ^{133}Cs removal at 0.15 M oxalic acid, and so experiments were conducted to find the optimal dosage and pH range of Ca(OH)$_2$ and NaTPB in 0.15 M oxalic acid washing wastewater. For the first step, in order to find the optimal dose of Ca(OH)$_2$ for cation removal, 15 mL of washing wastewater was mixed with various mass ratios from 0.1 to 1.2 g of Ca(OH)$_2$. As shown in Figure 6a, the concentrations of Al, Fe, Mg, and Si were analyzed for the largest amount of elution from HBT. Compared with the initial concentration, 63.26 mg/L of Mg remained in the solution, and other cations were removed to below 1 mg/L, when added at 0.0067 g/mL of Ca(OH)$_2$. Among the constituent elements of HBT, Mg ions are present in a high concentration in wastewater and occupy a large portion. However, at the 0.02 g/mL mass ratio of the Ca(OH)$_2$ dosage, the concentration of Al, Fe, and Mg in the wastewater was removed to below 0.1 mg/L, and Si decreased to 0.8 mg/L. Then, the pH in the solution was measured at 8.15. The Ca(OH)$_2$ dose above it showed a chemical equilibrium state, and the pH was maintained at 12.

As shown in the following reaction formula, when Ca(OH)$_2$ and NaTPB are added, the following reaction proceeds to remove metal ions and ^{133}Cs ions. (M: Metal ions; Ligand: Oxalic acid)

$$\text{M-Ligand Complex} + Ca(OH)_2 \rightarrow M(OH)_2\downarrow + \text{Ca-Ligand} \tag{1}$$

The metal removal mechanism by chemical precipitation is given in Equation (1). When Ca(OH)$_2$ is added to the washing wastewater complexed with dissolved metal ions and oxalate, the pH rises to basic conditions, and the metal-oxalate complex is converted to an insoluble hydroxide such as M(OH)$_2$ and precipitates. Metal ions are removed when the precipitate is separated through a PVDF membrane filter [45,46]. As a result, it was confirmed that in the condition of 0.15 M oxalic acid washing wastewater, Ca(OH)$_2$ was an optimal dosage of 0.02 g/mL, and the metal ions were almost removed when the pH was above 8.15. Figure 6b illustrates the concentration of heavy metal ions in the wastewater after the Cs desorption experiment. Knowing the concentrations is important because emission standards must be satisfied in order to discharge or dispose of the wastewater after completing all processes. As a result of the analysis, it was confirmed that Cr and Mn remained above 1 mg/L,

but both were below 0.1 mg/L after $Ca(OH)_2$ treatment. There have been a number of studies that used chemical precipitation methods to treat wastewater containing heavy metals. Cu^{2+}, Zn^{2+}, Cr^{3+} and Pb^{2+} ions were successfully removed by using fly ash as a seed material to enhance precipitation with lime [47]. They adjusted the pH value to 7–11 and succeeded in reducing the level of soluble heavy metals in the solution. In addition, Chen et al. (2012) found that metal ions can be successfully removed using $Ca(OH)_2$ from wastewater containing heavy metals. The removal efficiencies showed that the treatment effect was strongly dependent on the pH, and pH 10.5 was the optimal control point. In the pH region above 10.5, the removal efficiency of Mn^{2+} almost reached 100%, and Cd^{2+}, Zn^{2+}, Ni^{2+}, Cu^{2+} and Pb^{2+} precipitated from 90 to 99%, and the residual concentration was satisfied [46]. It is suggested that $Ca(OH)_2$ has a strong ability to remove heavy metals in wastewater. $Ca(OH)_2$ is better in complex wastewater than simulated single-metal wastewater, because a lot of precipitates are generated during the treatment process of complex wastewater.

Figure 6. (**a**) Determination of optimum conditions and pH changes for the removal of metal ions by $Ca(OH)_2$ dose in washing wastewater after 0.15 M oxalic acid treatment of HBT-[133]Cs contaminated clay minerals and (**b**) removal of heavy metal. (n = 2, mean ± standard error of mean).

3.5. Removal of Cs from Washing Wastewater of ^{133}Cs–HBT

In order to find the optimal dose of NaTPB, the cation-depleted 0.15 M oxalic acid washing wastewater and NaTPB were mixed at a mass ratio of 0.25 mg to 2.5 mg/mL and reacted overnight at 25 °C in a shaking incubator. As shown in Figure 7a, it was confirmed that the ^{133}Cs ions in the solution decreased as the NaTPB dose increased. In addition, when 2 mg and 2.5 mg NaTPB/10 mL solutions were added, ^{133}Cs ions were removed to below 0.68 mg/L and 0.46 mg/L, respectively. As shown in Figure 7b, in order to find the optimal pH range, various pH levels of oxalic acid washing wastewater were prepared from pH 1 to 13 and reacted by adding 20 mg of NaTPB to each 10 mL solution (wastewater).
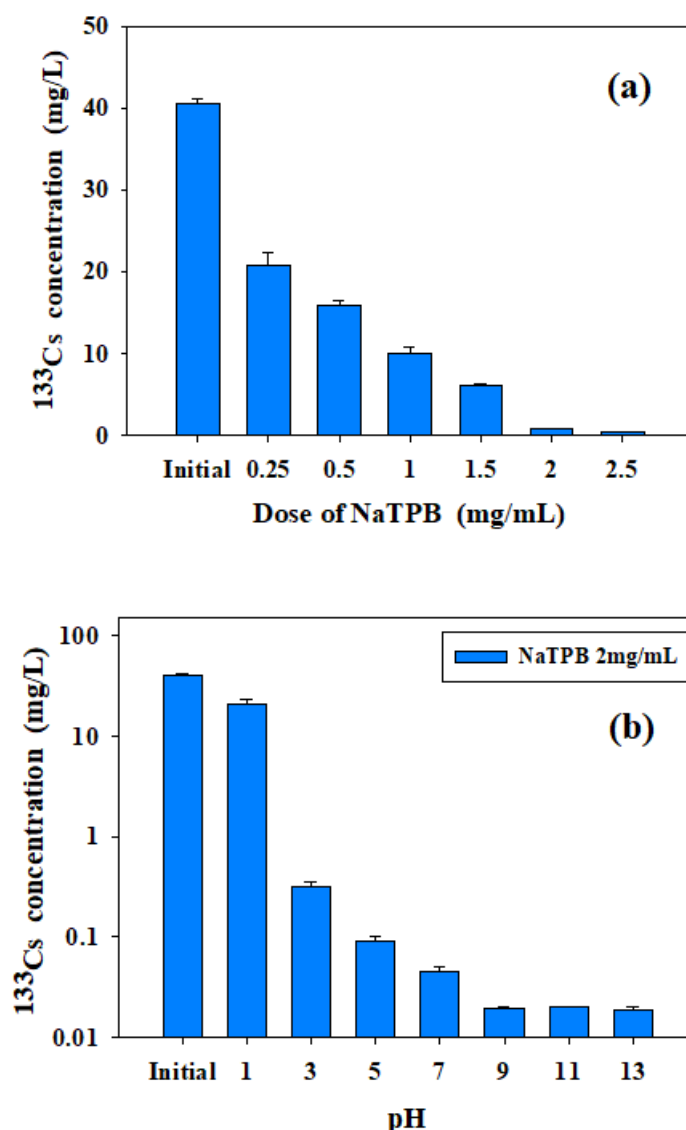
Figure 7. After treatment with 0.15 M oxalic acid from ^{133}Cs-HBT contaminated clay minerals, (**a**) the optimal dosage of NaTPB to remove ^{133}Cs ions from the washing wastewater (**b**) is in the optimal pH range. (n = 2, mean ± standard error of mean).

When the wastewater pH was 3, the Cs ions decreased below 1 mg/L, and the residual concentration of Cs was further removed from 0.05 to 0.02 mg/L while changing from pH 7 to 9. NaTPB has been known to quantitatively remove alkali metal ions such as Cs by forming insoluble salts [48–50].

The precipitation process with NaTPB, as shown in Equation (2), precipitates with CsTPB to remove Cs by solid/liquid separation using a PVDF membrane filter (pore size = 0.45 μm).

$$Na^+ + TPB^- + Cs^+ \rightarrow Na^+ + CsTPB\downarrow \qquad (2)$$

　　　Numerous previous studies reported that NaTPB forms poorly soluble CsTPB with Cs in aqueous solutions [51–53], thus providing a promising method for the removal of radiocesium from radioactive liquid waste. There are also many other precipitants for Cs removal, but CsTPB had the lowest K_{sp} (the solubility product, or K_{sp}, at 25 °C is 7.84×10^{-10} mol^2/L^2) of all cited. Based on this finding, NaTPB was used as a precipitating agent for Cs in this study. The CsTPB precipitate is typically in a form that is easily filtered [54]. Because not only CsTPB but also alkali metal salts (e.g., KTPB) are formed, a particularly high level of radioactivity causes radial decomposition of the TPB and environmentally harmful benzene is formed. Therefore, it must be separated as soon as it is formed [55]. Previous studies have reported the removal of Cs from radioactive wastewater using NaTPB. According to Kim et al. (2017), ash and soil contaminated with ^{137}Cs obtained from a nuclear facility were washed with HNO$_3$. NaTPB was used to remove ^{137}Cs from the generated wastewater. When treating the wastewater generated from contaminated ash, the initial concentration of ^{137}Cs was 3.2 Bq/g, and when NaTPB was added at a mass ratio of 7 mg/mL, it was reduced to 0.02 Bq/g. Additionally, the wastewater generated in contaminated soil showed that the initial concentration was 4.5 Bq/g, and this decreased to 0.04 Bq/g when treated with NaTPB 2 mg/mL mass ratio [56]. Another study by Rogers et al. (2012) reported that NaTPB and stable ^{133}Cs were treated in radioactive wastewater to reduce the initial concentration from 30 to 1.5 nCi/L [52]. Therefore, such previous studies support our results in that it is possible to selectively remove Cs with a high yield if NaTPB is adjusted to the optimal dosage and pH conditions in radioactive wastewater.

3.6. Application of Washing Wastewater Treatment

　　　In Figure 8, the optimum dose and pH conditions of Ca(OH)$_2$ and NaTPB we found were actually applied to the washing wastewater after the oxalic acid desorption experiment from 0.015 to 1.5 M concentration. In the first step, to remove cations from the desorption wastewater, Ca(OH)$_2$ was treated at a mass ratio of 0.025 g/mL, and in the second step, 2 mg/mL NaTPB was added to the cation-depleted wastewater in the previous step to remove Cs in the solution. As reflected in Figure 8b, in the first step, when the cations were compared with the initial concentration of Al, Fe, and Mg, these were removed to below 0.1 mg/L, and Si was reduced to below 1.1 mg/L in 0.2 M oxalic acid wastewater. Subsequently, as shown in Figure 8c, when the Ca(OH)$_2$ was treated, there was almost no change in the concentration of Cs, but it was confirmed that Cs was removed to below 0.1 mg/L in each wastewater sample when the NaTPB precipitant was treated.

　　　Therefore, we were able to confirm that the dosage and pH conditions of the precipitant were optimal through the results of this experiment. The ultimate goal is that the radioactive waste volume was reduced through a two-step precipitation method in the treatment of soil washing solution. First, the metal ions in the solution could be removed by primary precipitation, and Cs ions remaining in the solution were selectively precipitated by NaTPB, which resulted in the reduction of radioactive waste volume. Table 2 represents the dry weight of the precipitate after addition of Ca(OH)$_2$ and NaTPB, respectively. Under each optimal condition, 45 mg/mL of precipitate containing most metal ions was generated in the first step, and 2.4 mg/mL of precipitate with Cs ions (only 5% of the total precipitates) was generated in the second step. Therefore, it was confirmed that the amount of radioactive waste can be significantly reduced by separating metal ion precipitate and Cs ion precipitate. Figure 9 shows that Cs desorption in HBT is caused by hydrothermal treatment of oxalic acid due to the chelating effect and ion exchange from expanding between layers. In addition, the cation and Cs ions in washing wastewater were removed through a series of processes due to the hydroxide precipitation of M(OH)$_2$ and the chemical precipitation of CsTPB, respectively.
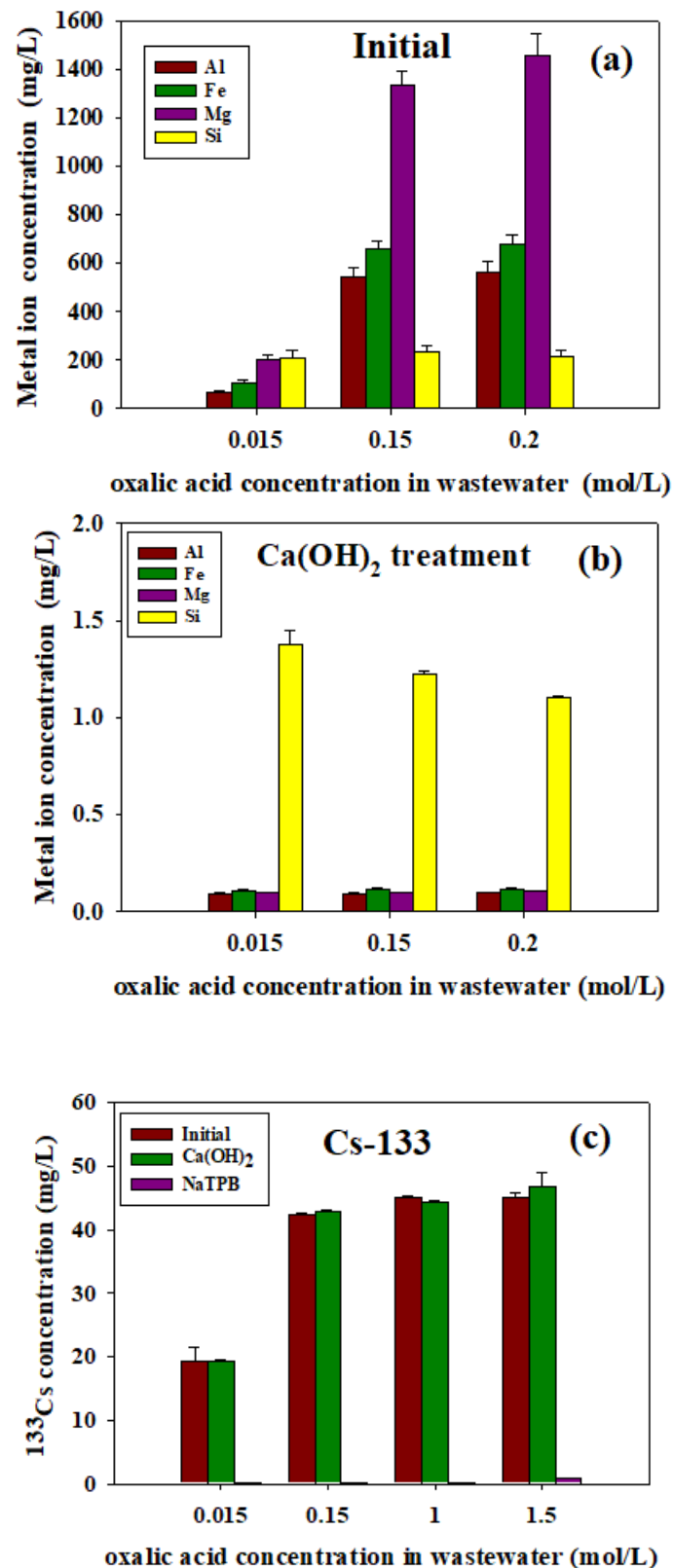
Figure 8. After the desorption experiment with oxalic acid at various concentrations: (**a**) the initial concentration of metal ions in the washing wastewater, (**b**) the concentration of cations after Ca(OH)$_2$ 0.025 g/mL treatment, and (**c**) the concentration of ^{133}Cs after 0.025 g/mL Ca(OH)$_2$ and 2 mg/mL NaTPB treatment. (n = 2, mean ± standard error of mean).

Table 2. Dry weight of precipitate after Ca(OH)$_2$ and NaTPB treatment.

Dry Weight of Precipitate after Ca(OH)$_2$ Treatment						
Dose of Ca(OH)$_2$ (mg/mL)	6.7	20 *	30	46	60	80
Dry weight (mg/mL)	14	45	54	56	73	99
Dry Weight of Precipitate after NaTPB Treatment						
Dose of NaTPB (mg/mL)	0.25	0.5	1	1.5	2 *	2.5
Dry weight (mg/mL)	0.4	0.62	0.121	1.61	2.37	2.78

* Optimal dose concentration (0.15 M oxalic acid wastewater).
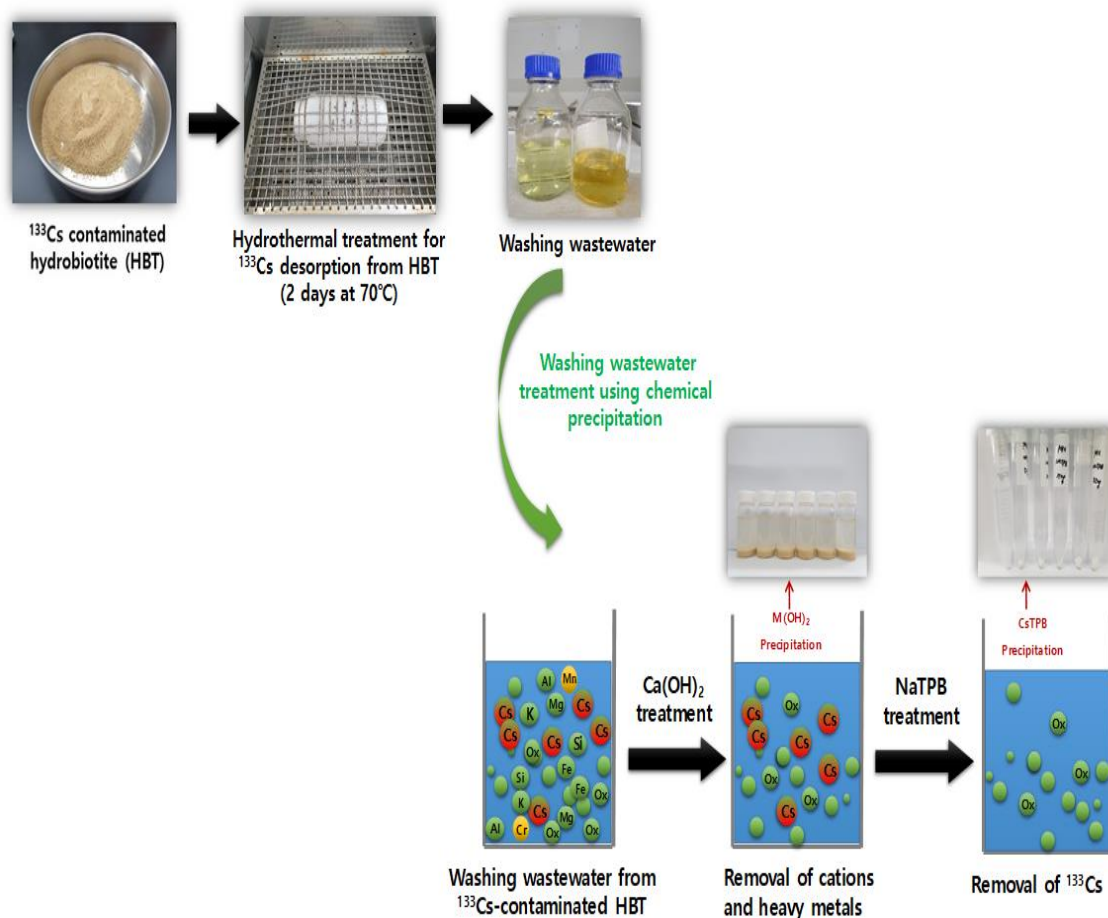
Figure 9. Process flowchart of removing Cs from contaminated [133]Cs–HBT and treating the remaining washing wastewater with chemical precipitation.

4. Conclusions

It is important to find the optimum conditions through a series of processes to remove Cs from radioactive contaminated soil (HBT) and to purify washing wastewater. We were able to decontaminate from Cs–HBT using oxalic acid, and both radioactive and non-radioactive experiments achieved removal efficiencies above 90% at a concentration of 0.15 M oxalic acid; the optimal desorption treatment conditions were found due to the attack of FES including Cs ions. Moreover, in the process of washing wastewater generated after the Cs removal tests, the optimum dosage and pH conditions for removing cations and Cs were found in the first step. In order to remove cations and heavy metal ions in the waste solution, Ca(OH)$_2$ was treated at a solid/solution ratio of 0.025 g/mL and optimum pH between 9 and 10. As a second step, to remove Cs, NaTPB was treated with a solid/solution ratio of

2 mg/mL, and Cs was removed to below 0.1 mg/L. These derived optimal conditions and treatment processes can be used as basic data to reduce the cost and the volume of radioactive waste and prevent environmental pollution when treating radioactive contaminated soil.

References

1. Lee, J.; Park, S.-M.; Jeon, E.-K.; Baek, K. Selective and irreversible adsorption mechanism of cesium on illite. *Appl. Geochem.* **2017**, *85*, 188–193. [CrossRef]

2. Wang, X.; Chen, L.; Wang, L.; Fan, Q.; Pan, D.; Li, J.; Chi, F.; Xie, Y.; Yu, S.; Xiao, C. Synthesis of novel nanomaterials and their application in efficient removal of radionuclides. *Sci. China Chem.* **2019**, *62*, 933–967. [CrossRef]

3. Rich, C.; Black, W. Pottasium exchange as affected by cation size, pH, and mineral structure. *Soil Sci.* **1964**, *97*, 384–390. [CrossRef]

4. Brouwer, E.; Baeyens, B.; Maes, A.; Cremers, A. Cesium and rubidium ion equilibriums in illite clay. *J. Phys. Chem.* **1983**, *87*, 1213–1219. [CrossRef]

5. Boettcher, A. Vermiculite, hydrobiotite, and biotite in the Rainy Creek igneous complex near Libby, Montana. *Clay Miner.* **1966**, *6*, 283–296. [CrossRef]

6. Brindley, G.; Zalba, P.E.; Bethke, C.M. Hydrobiotite, a regular 1: 1 interstratification of biotite and vermiculite layers. *Am. Mineral.* **1983**, *68*, 420–425.

7. Yamada, H.; Yokoyama, S.; Watanabe, Y.; Suzuki, M.; Suzuki, S.; Hatta, T. Cesium-adsorption Behavior of Weathered Biotite from Fukushima Prefecture Depends on the Degree of Vermiculitization. *J. Ion. Exch.* **2014**, *25*, 207–211. [CrossRef]

8. Nakao, A.; Thiry, Y.; Funakawa, S.; Kosaki, T. Characterization of the frayed edge site of micaceous minerals in soil clays influenced by different pedogenetic conditions in Japan and northern Thailand. *Soil Sci. Plant Nutr.* **2008**, *54*, 479–489. [CrossRef]

9. Mukai, H.; Motai, S.; Yaita, T.; Kogure, T. Identification of the actual cesium-adsorbing materials in the contaminated Fukushima soil. *Appl. Clay Sci.* **2016**, *121*, 188–193. [CrossRef]

10. Dzene, L.; Tertre, E.; Hubert, F.; Ferrage, E. Nature of the sites involved in the process of cesium desorption from vermiculite. *J. Colloid Interface Sci.* **2015**, *455*, 254–260. [CrossRef]

11. Mukai, H.; Hirose, A.; Motai, S.; Kikuchi, R.; Tanoi, K.; Nakanishi, T.M.; Yaita, T.; Kogure, T. Cesium adsorption/desorption behavior of clay minerals considering actual contamination conditions in Fukushima. *Sci. Rep.* **2016**, *6*, 1–7. [CrossRef]

12. Tan, K.H. *Principles of Soil Chemistry*; CRC Press: Boca Raton, FL, USA, 2010.

13. Sanjay, G.; Sugunan, S. Acid activated montmorillonite: An efficient immobilization support for improving reusability, storage stability and operational stability of enzymes. *J. Porous Mater.* **2008**, *15*, 359–367. [CrossRef]

14. Berner, R.A.; Holdren Jr, G.R. Mechanism of feldspar weathering—II. Observations of feldspars from soils. *Geochim. Et Cosmochim. Acta* **1979**, *43*, 1173–1186. [CrossRef]

15. Kim, B.H.; Park, C.W.; Yang, H.-M.; Seo, B.-K.; Lee, B.-S.; Lee, K.-W.; Park, S.J. Comparison of Cs desorption from hydrobiotite by cationic polyelectrolyte and cationic surfactant. *Colloids Surf. A Physicochem. Eng. Asp.* **2017**, *522*, 382–388. [CrossRef]

16. Jolin, W.C.; Kaminski, M.J.C. Sorbent materials for rapid remediation of wash water during radiological event relief. *Chemosphere* **2016**, *162*, 165–171. [CrossRef] [PubMed]

17. Zaheri, A.; Moheb, A.; Keshtkar, A.; Shirani, A. Uranium separation from wastewater by electrodialysis. *J. Environ. Health Sci. Eng.* **2010**, *7*, 423–430.

18. Chmielewski, A.; Harasimowicz, M.; Zakrzewska-Trznadel, G. Membrane technologies for liquid radioactive waste treatment. *Czechoslov. J. Phys.* **1999**, *49*, 979–985. [CrossRef]

19. Ku, Y.; Jung, I.-L. Photocatalytic reduction of Cr (VI) in aqueous solutions by UV irradiation with the presence of titanium dioxide. *Water Res.* **2001**, *35*, 135–142. [CrossRef]

20. Huisman, J.L.; Schouten, G.; Schultz, C. Biologically produced sulphide for purification of process streams, effluent treatment and recovery of metals in the metal and mining industry. *Hydrometallurgy* **2006**, *83*, 106–113. [CrossRef]

21. Park, C.W.; Kim, B.H.; Yang, H.-M.; Seo, B.-K.; Lee, K.-W. Enhanced desorption of Cs from clays by a polymeric cation-exchange agent. *J. Hazard. Mater.* **2017**, *327*, 127–134. [CrossRef]

22. Komadel, P.; Madejová, J. Acid activation of clay minerals. In *Developments in Clay Science*; Elsevier: Amsterdam, The Netherlands, 2013; Volume 5, pp. 385–409.

23. Krupskaya, V.; Zakusin, S.; Tyupina, E.; Dorzhieva, O.; Zhukhlistov, A.; Belousov, P.; Timofeeva, M. Experimental study of montmorillonite structure and transformation of its properties under treatment with inorganic acid solutions. *Minerals* **2017**, *7*, 49. [CrossRef]

24. Al-Essa, K. Activation of Jordanian bentonite by hydrochloric acid and its potential for olive mill wastewater enhanced treatment. *J. Chem.* **2018**, *2018*, 1–10. [CrossRef]

25. Malmström, M.; Banwart, S.; Lewenhagen, J.; Duro, L.; Bruno, J. The dissolution of biotite and chlorite at 25 C in the near-neutral pH region. *J. Contam. Hydrol.* **1996**, *21*, 201–213. [CrossRef]

26. Malmström, M.; Banwart, S. Biotite dissolution at 25 C: The pH dependence of dissolution rate and stoichiometry. *Geochim. Et Cosmochim. Acta* **1997**, *61*, 2779–2799. [CrossRef]

27. Liu, C.; Zachara, J.M.; Smith, S.C.; McKinley, J.P.; Ainsworth, C.C. Desorption kinetics of radiocesium from subsurface sediments at Hanford Site, USA. *Geochim. Et Cosmochim. Acta* **2003**, *67*, 2893–2912. [CrossRef]

28. Kim, G.-N.; Choi, W.-K.; Jung, C.-H.; Moon, J.-K. Development of a washing system for soil contaminated with radionuclides around TRIGA reactors. *J. Ind. Eng. Chem.* **2007**, *13*, 406–413.

29. Wendling, L.A.; Harsh, J.B.; Palmer, C.D.; Hamilton, M.A.; Flury, M. Cesium sorption to illite as affected by oxalate. *Clays Clay Miner.* **2004**, *52*, 375–381. [CrossRef]

30. Sawhney, B. Potassium and cesium ion selectivity in relation to clay mineral structure. *Clays Clay Miner.* **1970**, *18*, 47–52. [CrossRef]

31. Sawhney, B. Selective sorption and fixation of cations by clay minerals: A review. *Clays Clay Miner.* **1972**, *20*, 93–100. [CrossRef]

32. Kim, Y.; Kim, K.; Kang, H.-D.; Kim, W.; Doh, S.-H.; Kim, D.-S.; Kim, B.-K. The accumulation of radiocesium in coarse marine sediment: Effects of mineralogy and organic matter. *Mar. Pollut. Bull.* **2007**, *54*, 1341–1350. [CrossRef]

33. Xavier, K.C.M.; Santos, M.d.S.F.d.; Santos, M.R.M.C.; Oliveira, M.E.R.; Carvalho, M.W.N.C.; Osajima, J.A.; Silva Filho, E.C.d. Effects of acid treatment on the clay palygorskite: XRD, surface area, morphological and chemical composition. *Mater. Res.* **2014**, *17*, 3-08. [CrossRef]

34. Wang, X.; Li, Q.; Hu, H.; Zhang, T.; Zhou, Y. Dissolution of kaolinite induced by citric, oxalic, and malic acids. *J. Colloid Interface Sci.* **2005**, *290*, 481–488. [CrossRef] [PubMed]

35. Fein, J.B.; Hestrin, J.E. Experimental studies of oxalate complexation at 80 C: Gibbsite, amorphous silica, and quartz solubilities in oxalate-bearing fluids. *Geochim. Et Cosmochim. Acta* **1994**, *58*, 4817–4829. [CrossRef]

36. Welch, S.A.; Ullman, W.J. The temperature dependence of bytownite feldspar dissolution in neutral aqueous solutions of inorganic and organic ligands at low temperature (5–35 C). *Chem. Geol.* **2000**, *167*, 337–354. [CrossRef]

37. Surdam, R.C.; Boese, S.W.; Crossey, L.J. The chemistry of secondary porosity: Part 2. Aspects of porosity modification. *Calstic Diagenesis* **1984**, 127–149. Available online: archives.datapages.com/data/specpubs/sandsto2/data/a059/0001/0100/0127.htm (accessed on 13 May 2020).

38. Huang, W.; Kiang, W. Laboratory dissolution of plagioclase feldspars in water and organic acids at room temperature. *Am. Mineral. J. Earth Planet. Mater.* **1972**, *57*, 1849–1859.

39. Mukai, H.; Tamura, K.; Kikuchi, R.; Takahashi, Y.; Yaita, T.; Kogure, T. Cesium desorption behavior of weathered biotite in Fukushima considering the actual radioactive contamination level of soils. *J. Environ. Radioact.* **2018**, *190*, 81–88. [CrossRef]

40. Murakami, T.; Utsunomiya, S.; Yokoyama, T.; Kasama, T. Biotite dissolution processes and mechanisms in the laboratory and in nature: Early stage weathering environment and vermiculitization. *Am Mineral.* **2003**, *88*, 377–386. [CrossRef]

41. Turpault, M.-P.; Trotignon, L. The dissolution of biotite single crystals in dilute HNO3 at 24 C: Evidence of an anisotropic corrosion process of micas in acidic solutions. *Geochim. Et Cosmochim. Acta.* **1994**, *58*, 2761–2775. [CrossRef]

42. Kalinowski, B.E.; Schweda, P. Kinetics of muscovite, phlogopite, and biotite dissolution and alteration at pH 1–4, room temperature. *Geochim. Et Cosmochim. Acta.* **1996**, *60*, 367–385. [CrossRef]

43. Murakami, T.; Ito, J.-I.; Utsunomiya, S.; Kasama, T.; Kozai, N.; Ohnuki, T. Anoxic dissolution processes of biotite: Implications for Fe behavior during Archean weathering. *Earth Planet. Sci. Lett.* **2004**, *224*, 117–129. [CrossRef]

44. Zhong, S.; Sun, S.; Chen, T.; Peng, S.J. Influence of hydrochloric acid-dissolution on the structure of montmorillonite. *J. Chi. Ceram. Soc.* **2006**, *34*, 1162.

45. Wang, L.K.; Vaccari, D.A.; Li, Y.; Shammas, N.K. Chemical precipitation. In *Physicochemical Treatment Processes*; Springer: Berlin, Germany, 2005; pp. 141–197.

46. Chen, B.; Qu, R.; Shi, J.; Li, D.; Wei, Z.; Yang, X.; Wang, Z. Heavy metal and phosphorus removal from waters by optimizing use of calcium hydroxide and risk assessment. *Environ. Pollut.* **2012**, *1*, 38. [CrossRef]

47. Chen, Q.; Luo, Z.; Hills, C.; Xue, G.; Tyrer, M. Precipitation of heavy metals from wastewater using simulated flue gas: Sequent additions of fly ash, lime and carbon dioxide. *Water Res.* **2009**, *43*, 2605–2614. [CrossRef] [PubMed]

48. Rüdorff, W.; Zannier, H. Argentometrie von Kalium und organischen N-haltigen Basen mit Natrium-tetraphenyloborat. *Angew. Chem.* **1954**, *66*, 638–639. [CrossRef]

49. Amin, A.-A.M. Determination of Ammonium, Potassium, Rubidium, or Cesium via Cationic Resin Exchange of Their Tetraphenylboron Salts. *Chem. Anal* **1956**, *45*, 65.

50. Ponder, S.M.; Mallouk, T.E. Recovery of ammonium and cesium ions from aqueous waste streams by sodium tetraphenylborate. *Ind. Eng. Chem. Res.* **1999**, *38*, 4007–4010. [CrossRef]

51. Lee, E.-H.; Lim, J.-G.; Chung, D.-Y.; Yang, H.-B.; Kim, K.-W. Selective removal of Cs and Re by precipitation in a Na2CO3–H2O2 solution. *J. Radioanal. Nucl. Chem.* **2010**, *284*, 387–395. [CrossRef]

52. Rogers, H.; Bowers, J.; Gates-Anderson, D. An isotope dilution–precipitation process for removing radioactive cesium from wastewater. *J. Hazard. Mater.* **2012**, *243*, 124–129. [CrossRef]

53. Soliman, M.A.; Rashad, G.M.; Mahmoud, M.R. Fast and efficient cesium removal from simulated radioactive liquid waste by an isotope dilution–precipitate flotation process. *Chem. Eng. J.* **2015**, *275*, 342–350. [CrossRef]

54. Council, N.R. *Alternatives for High-Level Waste Salt Processing at the Savannah River Site*; National Academies Press: Washington, DC, USA, 2000.

55. Gupta, A.K.; Hanrahan, R.J.; Walker, D.D. Radiolysis of sodium and potassium tetraphenylborate in aqueous systems. *J. Phys. Chem.* **1991**, *95*, 3590–3594. [CrossRef]

56. Kim, G.-N.; Kim, S.-S.; Choi, J.-W. Development of an agent suited for adsorbing Cs-137 from ash and soil waste solutions. *Sep. Purif. Technol.* **2017**, *173*, 193–199. [CrossRef]